Observation of Conformal Symmetry Breaking and Scale Invariance in Expanding Fermi Gases

E. Elliott,[1,2] J. A. Joseph,[1] and J. E. Thomas[1*]
[1]Department of Physics, North Carolina State University, Raleigh, North Carolina 27695, USA
[2]Department of Physics, Duke University, Durham, North Carolina 27708, USA

(Received 18 October 2013; revised manuscript received 18 December 2013; published 29 January 2014)

We precisely test scale invariance and examine local thermal equilibrium in the hydrodynamic expansion of a Fermi gas of atoms as a function of interaction strength. After release from an anisotropic optical trap, we observe that a resonantly interacting gas obeys scale-invariant hydrodynamics, where the mean square cloud size $\langle \mathbf{r}^2 \rangle = \langle x^2 + y^2 + z^2 \rangle$ expands ballistically (like a noninteracting gas) and the energy-averaged bulk viscosity is consistent with zero, $0.00(0.04)\hbar n$, with n the density. In contrast, the aspect ratios of the cloud exhibit anisotropic "elliptic" flow with an energy-dependent shear viscosity. Tuning away from resonance, we observe conformal symmetry breaking, where $\langle \mathbf{r}^2 \rangle$ deviates from ballistic flow.

DOI: 10.1103/PhysRevLett.112.040405 PACS numbers: 03.75.Ss

The identification and comparison of scale-invariant physical systems, defined as those without an intrinsic length scale, has enabled significant advances connecting diverse fields of physics. Of recent interest are connections between scale-invariant strongly interacting systems and their weakly interacting counterparts. An important example is the anti–de Sitter-conformal field theory correspondence, which provides a geometric link between a broad class of scale-invariant (conformal) strongly interacting quantum fields and their weakly interacting gravitational field counterparts in five dimensions [1]. In the weakly interacting representation, both the shear viscosity η and the entropy density s are found to be proportional to the surface area of a black hole. The surface area therefore cancels in the ratio η/s, enabling a prediction of a universal lower bound for η/s in strongly interacting systems [2]. This prediction connects quark-gluon plasmas [3,4] to ultracold Fermi gases, which have nearly identical η/s ratios, just a few times the lower bound, despite differing in temperature by 19 orders of magnitude and in density by 25 orders of magnitude [1,5–7]. An ultracold Fermi gas is a paradigm for scale-invariant quantum fluids with the unique trait that a cloud of spin-up and spin-down atoms is magnetically tunable between scale-invariant strongly interacting and noninteracting fluids. The development of nonrelativistic conformal field theory [8] may expose a deep geometric correspondence between these two regimes.

Near a collisional (Feshbach) resonance, the s-wave scattering length a_S for interactions between spin-up and spin-down atoms can be tuned to a zero crossing, where $a_S = 0$ and the gas is noninteracting. Tuning to resonance, where a_S diverges, the cloud is the most strongly interacting, nonrelativistic quantum system known [9]. A central connection between these two regimes is that in both cases, the thermal equilibrium pressure p and energy density $\mathcal{E}$ are related by $p = (2/3)\mathcal{E}$, which follows from the universal hypothesis [10,11]. This equation of state for a resonantly interacting Fermi gas has been verified experimentally to high precision [12], but only for a trapped gas. An obvious distinction between the ideal and strongly interacting regimes was first demonstrated by observing the aspect ratio of a Fermi gas after release from an anisotropic trap [13]. The ideal gas was shown to expand ballistically with an isotropic momentum distribution, whereas the strongly interacting gas was found to expand hydrodynamically and to exhibit anisotropic "elliptic" flow [3,13].

In this Letter, we demonstrate both theoretically and experimentally that scale invariance connects the resonantly interacting and ideal noninteracting gas by requiring the mean square cloud size $\langle \mathbf{r}^2 \rangle = \langle x^2 + y^2 + z^2 \rangle$ to expand identically, in contrast to the aspect ratios. Tuning the cloud away from resonance, where the scattering length is finite, we observe breaking of scale invariance, which is controlled by the conformal symmetry breaking pressure $\Delta p \equiv p - (2/3)\mathcal{E}$ and the bulk viscosity. We

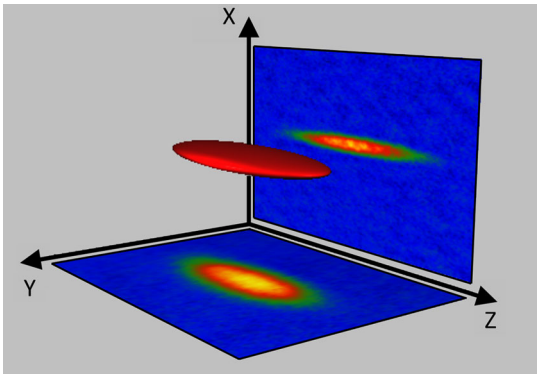

FIG. 1 (color online). Imaging the expanding cloud in three dimensions. Two CCD cameras are used to measure the density profile of the cloud. The cloud is released from an asymmetric optical trap with a 1.0:2.7:33 (x:y:z) aspect ratio, enabling observation of elliptic flow in the x-y plane.

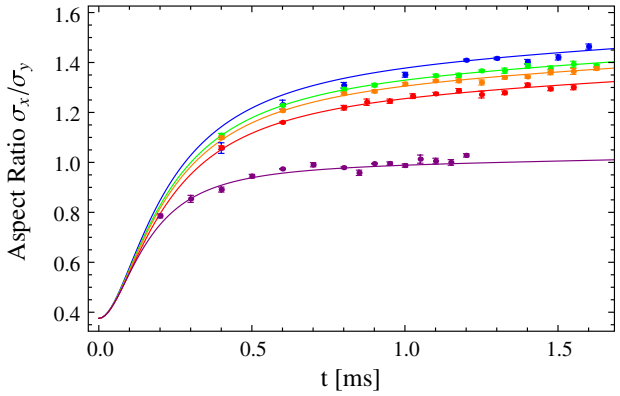

FIG. 2 (color online). Transverse aspect ratio σ_x/σ_y versus time after release showing elliptic hydrodynamic flow: Top to bottom, resonantly interacting gas at 834 G, $\tilde{E} = 0.66E_F$, $\tilde{E} = 0.89E_F$, $\tilde{E} = 1.17E_F$, $\tilde{E} = 1.46E_F$, ballistic (noninteracting) gas at 528 G, $\tilde{E} = 1.78E_F$. Top four solid curves: Hydrodynamic theory with the shear viscosity as the only fit parameter. Lower solid curve: Ballistic theory with no free parameters. Error bars denote statistical fluctuations in the aspect ratio.

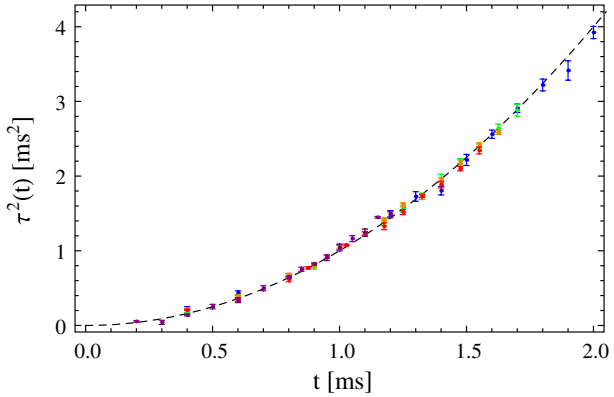

FIG. 3 (color online). Scale invariant expansion of a resonantly interacting Fermi gas. Experimental values of $\tau^2(t) \equiv m[\langle \mathbf{r}^2\rangle - \langle \mathbf{r}^2\rangle_0]/\langle \mathbf{r}\cdot\nabla U\rangle_0$ versus time t after release, for the same data as in Fig. 2 (including noninteracting gas data) collapse onto a single curve, demonstrating universal t^2 scaling. Dashed curve $\tau^2(t) = t^2$, as predicted by Eq. (2) [22].

show that measurement of $\langle \mathbf{r}^2\rangle = \langle x^2 + y^2 + z^2\rangle$ enables a precision measurement of the bulk viscosity without creating a spherical trap and tests local thermal equilibrium during expansion.

In the experiments, we employ an optically trapped cloud of ^{6}Li atoms in a 50-50 mixture of the two lowest hyperfine states, which is cooled by evaporation [13] to temperatures in the normal fluid regime between $T/T_{\rm FI} = 0.2$ to 0.6, where $k_B T_{\rm FI} = E_F$ and E_F is the Fermi temperature of an ideal Fermi gas at the trap center [14]. We determine $\tilde{E} \equiv \langle \mathbf{r}\cdot\nabla U\rangle_0$ from the trapped cloud profile and use it as an interaction-independent initial energy scale [14]. The cloud is released from an anisotropic trap with a 1:2.7:33 aspect ratio. Two independent images, Fig. 1, are obtained using two CCD cameras and two simultaneous, orthogonally propagating probe beam pulses, which each interact with a different hyperfine state. In this way, the cloud profile is measured as a function of time after release in all three dimensions.

We relate the acceleration of the mean square cloud radius to the conformal symmetry breaking pressure Δp and the bulk viscosity ζ_B, using the hydrodynamic equation for the velocity field $\mathbf{v}$ (including pressure and viscous forces) and the continuity equation for the density n, which are consistent with energy conservation. *Without* assuming a scaling solution, we find that a single-component fluid comprising N atoms of mass m obeys [14]

$$\frac{d^2}{dt^2}\frac{m\langle \mathbf{r}^2\rangle}{2} = \langle \mathbf{r}\cdot\nabla U_{\rm opt}\rangle_0 + \frac{3}{N}\int d^3\mathbf{r}\,[\Delta p - \Delta p_0] - \frac{3}{N}\int d^3\mathbf{r}\,\zeta_B \nabla\cdot\mathbf{v}, \quad (1)$$

where the subscript $(_0)$ denotes the condition at $t = 0$, just after the optical trap is extinguished and ζ_B is the local bulk viscosity. For brevity, we include only the optical trap potential $U_{\rm opt}$ in Eq. (1), which need not be harmonic. However, for the analysis of our precision measurements, we also include the small potential energy arising from the finite curvature of the bias magnetic field [14]. As $\langle \mathbf{r}^2\rangle$ is a scalar, the contribution of the shear viscosity pressure tensor vanishes, since it is traceless.

The aspect ratio σ_x/σ_y of the cloud is measured at the ^{6}Li Feshbach resonance at 834 G [15,16] as a function of time after release to establish that the flow is hydrodynamic and to determine the shear viscosity. Figure 2 shows data for $\tilde{E}/E_F = 0.66$, 0.89, 1.17, 1.46. The hydrodynamic expansion data at 834 G is compared to that of a noninteracting gas taken at 528 G where $a_S = 0$ and $\tilde{E}/E_F = 1.78$. For the noninteracting gas, which expands ballistically, the aspect ratio saturates to unity. In contrast, for the resonantly interacting cloud, σ_x/σ_y increases to approximately 1.5 over the time range shown, clearly demonstrating that the cloud expands hydrodynamically. The shear viscosity increases with increasing energy (see Fig. 5), slowing down the rate at which the aspect ratio increases with time.

For a resonantly interacting cloud, important questions are whether $\Delta p = p - (2/3)\mathcal{E}$ remains zero during expansion and if the expansion is scale invariant. The bulk viscosity ζ_B is predicted to vanish in the scale-invariant regime [17–20], consistent with the bulk viscosity frequency sum rule, which vanishes when $\Delta p = 0$ [21]. If these conditions hold, Eq. (1) yields

$$\langle \mathbf{r}^2\rangle = \langle \mathbf{r}^2\rangle_0 + \frac{t^2}{m}\langle \mathbf{r}\cdot\nabla U_{\rm opt}\rangle_0, \quad (2)$$

which corresponds to ballistic expansion of the mean square cloud size (in the same way as a noninteracting

gas), even though the individual cloud radii expand hydrodynamically and exhibit elliptic flow, as shown in Fig. 2 for the transverse aspect ratio.

Scale invariance of the expanding gas is now directly tested by determining $\tau^2(t) \equiv m[\langle \mathbf{r}^2 \rangle - \langle \mathbf{r}^2 \rangle_0]/\langle \mathbf{r} \cdot \nabla U_{\rm opt} \rangle_0$ from the measured cloud radii and the trap parameters [14]. By construction, $\tau^2(t)$ will be independent of the initial cloud size and should obey $\tau^2(t) = t^2$, according to Eq. (2), if the system is scale invariant. Figure 3 shows the experimental values of $\tau^2(t)$ versus t for the same data as used in Fig. 2, including the noninteracting gas data. In contrast to the aspect ratio versus time data of Fig. 2, which varies substantially with energy due to the shear viscosity, the combined $\tau^2(t)$ data fall on a t^2 curve with $\chi^2 = 1.1$ using no free parameters. This is consistent with $\Delta p = 0$ and scale invariant expansion, which suggests that the equation of state $p = (2/3)\mathcal{E}$ and, hence, local thermodynamic equilibrium, are maintained in the hydrodynamic expansion. Further, these results directly demonstrate that scale invariance is not destroyed by shear viscosity, which therefore may be amenable to study in Fermi gases by scale invariant (conformal) field theory methods [8].

We investigate the breaking of scale invariance for the expanding gas at finite scattering length by tuning the bias magnetic field above and below the Feshbach resonance. Figure 4 shows $\tau^2(t)$ data for $\tilde{E} \simeq 1.0 E_F$. Compared to the resonant case, we see qualitatively that the cloud expands more rapidly when the scattering length is negative $1/(k_{\rm FI} a_S) = -0.59$ and more slowly when the scattering length is positive, $1/(k_{\rm FI} a_S) = +0.61$, where $k_{\rm FI} = \sqrt{2mE_F}/\hbar$. This behavior is a signature of the $[\Delta p - \Delta p_0]$ term in Eq. (1), where $|\Delta p(t)| \leq |\Delta p(0)|$ for any time t after release and Δp has the same sign as the scattering length.

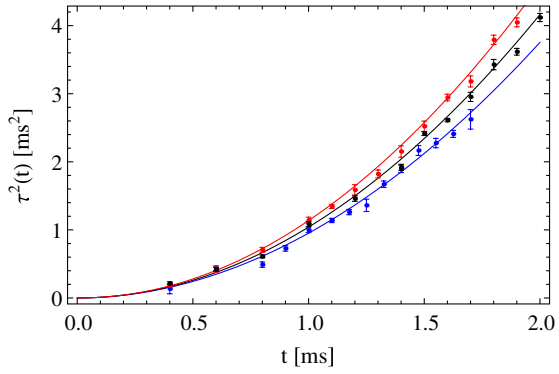

FIG. 4 (color online). Conformal symmetry breaking in the expansion for a Fermi gas near a Feshbach resonance. The data are the experimental values of $\tau^2(t) \equiv m[\langle \mathbf{r}^2 \rangle - \langle \mathbf{r}^2 \rangle_0]/\langle \mathbf{r} \cdot \nabla U \rangle_0$ for $\tilde{E}/E_F \simeq 1.0$, versus time t after release. Solid curves are the predictions using Eq. (1) with $\zeta_B = 0$, where the pressure change Δp is approximated using the second virial coefficient without any free parameters [14]. Top: $1/(k_{\rm FI} a_S) = -0.59$; Center: $1/(k_{\rm FI} a_S) = 0$; Bottom: $1/(k_{\rm FI} a_S) = +0.61$.

To estimate $\Delta p - \Delta p_0$ in Eq. (1), we employ for simplicity a high-temperature, second virial coefficient approximation [23]. We retain only the translational degrees of freedom and ignore the contribution from changes in the molecular population, which require three-body collisions that occur with low probability during the expansion time scale. In Δp, the translational temperature is evaluated using an adiabatic approximation, so that $\Delta p(t)$ is then a known function of time and is odd in $1/a_S$ [14]. We find that estimating Δp in this way yields satisfactory agreement with the data of Fig. 4, even for relatively low energies $\tilde{E}/E_F \simeq 1$. The reasonable fits suggests that two-body interactions are dominant for $1/(k_{\rm FI} a_S) \simeq \pm 0.6$. The expansion at finite $1/a_S$ is energy dependent, since Δp approaches zero as the energy is increased [14].

We present a new precision measurement of the shear viscosity at resonance, which serves as a reference for the bulk viscosity measurement described below. This is accomplished by measuring the *transverse* aspect ratio as a function of time after release, Fig. 2. The shear viscosity pressure tensor slows the flow in the rapidly expanding, initially narrow, x direction and increases the speed in the more slowly expanding y direction. As the initial transverse aspect ratio is 1:2.7 for our trap, elliptic flow is observed for relatively short expansion times with high signal to background ratio, enabling high sensitivity to the shear viscosity, even at the lowest energies, which were not accessible in our previous expansion measurements [6,7]. We fit the data of Fig. 2 for a resonantly interacting gas at 834 G, using a general, energy-conserving, hydrodynamic model [6,7], valid in the scale-invariant regime where $\Delta p = 0$. At resonance, the shear viscosity η takes the form $\eta = \alpha_S \hbar n$, where n is the total density of atoms and α_S is a dimensionless function of the local reduced temperature. The trap-averaged shear viscosity

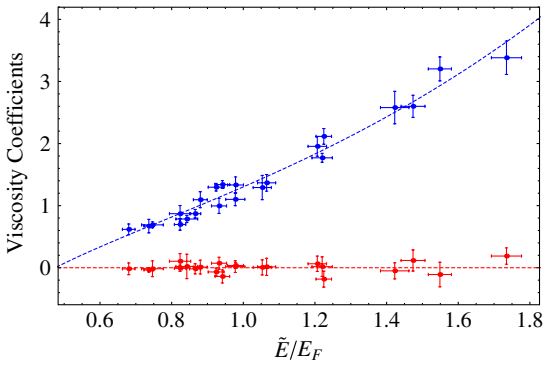

FIG. 5 (color online). Measurement of bulk and shear viscosity for a scale-invariant Fermi gas: Blue (top): Trap-averaged shear viscosity coefficient $\int d^3\mathbf{r}\eta/(N\hbar) \equiv \bar{\alpha}_S$ versus energy $\tilde{E}/E_F$. Red (bottom): Trap-averaged bulk viscosity coefficient $\int d^3\mathbf{r}\zeta_B/(N\hbar) \equiv \bar{\alpha}_B$ versus energy. Bars denote statistical error. (Dashed curves added to guide the eye.)

coefficient $\bar{\alpha}_S \equiv \int d^3\mathbf{r}\,\eta/(\hbar N)$ is used as the only free parameter, initially neglecting the bulk viscosity, which is expected to be much smaller. For the shear viscosity in the scale-invariant regime, $\bar{\alpha}_S$ is an adiabatic invariant, which is therefore temporally constant in the adiabatic approximation [6,7]. The fits to the aspect ratio obtained in this way are shown in Fig. 2 as solid lines and yield the data shown in Fig. 5.

The bulk viscosity is measured with high sensitivity from the expansion of $\langle \mathbf{r}^2 \rangle$, Eq. (1), which is independent of the shear viscosity. The divergence of the velocity field $\mathbf{v}$ is easily determined from the fits to the aspect ratios using a scaling approximation, which is adequate for the small bulk viscosity term. Figure 3 shows that both Δp and ζ_B must be nearly zero. To estimate the bulk viscosity at resonance, we assume that $\Delta p = p - (2/3)\mathcal{E} = 0$ for the expanding, resonantly interacting gas, so that the bulk viscosity term in Eq. (1) produces the only deviation from scale invariance in the evolution of $\langle \mathbf{r}^2 \rangle$.

Analogous to the shear viscosity, we take the bulk viscosity to be of the form $\zeta_B = \alpha_B \hbar n$, where α_B is dimensionless, and consider first a large finite scattering length. Since the bulk viscosity must be positive, the leading contribution in powers of the inverse scattering length a_S must be of the form $\zeta_B = f_B(\theta)\hbar n/(k_F a_S)^2$, where $k_F = (3\pi^2 n)^{1/3}$ is the local Fermi wave vector. Here, $f_B(\theta)$ is a dimensionless function of the reduced temperature θ, which is an adiabatic invariant, and, hence, time independent in the adiabatic approximation that we use for the small bulk viscosity contribution. As the cloud expands, the density decreases as $n \propto 1/\Gamma$ in the scaling approximation, where the fits to the aspect ratio data in all three dimensions accurately determine the volume scale factor $\Gamma(t)$ [14]. Since $1/k_F^2 \propto \Gamma^{2/3}$, the trap-averaged bulk viscosity coefficient $\bar{\alpha}_B \equiv \int d^3\mathbf{r}\zeta_B/(\hbar N)$ is time dependent and scales as

$$\bar{\alpha}_B(t) = \bar{\alpha}_B(0)\,\Gamma^{2/3}(t). \tag{3}$$

With the scaling approximation $\nabla \cdot \mathbf{v} = \dot{\Gamma}/\Gamma$, the bulk viscosity term then takes the simple form $-3\hbar\bar{\alpha}_B(0)\dot{\Gamma}/\Gamma^{1/3}$. We determine $\bar{\alpha}_B(0)$ with high precision by using a least-squares fit of Eq. (1) to the measured $\langle \mathbf{r}^2 \rangle$ data [14]. In contrast to the shear viscosity coefficient, which increases with increasing energy, Fig. 5 shows that the bulk viscosity coefficient at resonance remains nearly zero over the entire energy range. We find that the weighted average $\bar{\alpha}_B(0) = 0.00(0.04)$, is consistent with zero, as predicted for a scale-invariant cloud [17–20]. The error estimate includes both statistical and systematic contributions. We correct the optical trapping potential for anharmonicity, which is measured from the expansion of a noninteracting gas [14]. The quadrupolar potential arising from the bias magnetic field curvature [14] produces a maximum 1.5% change in $\langle \mathbf{r}^2 \rangle$ at the longest release times. We include this in the theory to eliminate the corresponding systematic error. We note that the most recent precision determination of the broad Feshbach resonance in ^{6}Li places it at 832.2 G [16], 2 G below the 834 G value we employ. Using the high temperature approximations for Δp, and a zero temperature approximation valid to leading order in $1/(k_{\mathrm{FI}} a_S)$, we find that a 2 G offset produces a maximum systematic change in $\bar{\alpha}_B(0)$ of 0.005, well within our error estimate. By an order of magnitude, the systematic error in $\bar{\alpha}_B(0)$ is dominated by the uncertainty in ω_z [14]. The null result for the bulk viscosity is 2 orders of magnitude more stringent than that obtained from our previous consistency argument [7], where only one relatively high energy ($E/E_F \simeq 3.3$) was studied with low sensitivity, by measuring the expansion of the aspect ratio.

We also estimate the bulk viscosity for finite $1/a_S$. From Fig. 4, we see that Δp, which is an odd function of $1/a_S$, adequately accounts for most of the deviation from scale invariant ballistic expansion. A nonzero bulk viscosity would shift both finite a_S curves downward. In a more detailed analysis [14], we fit the data for finite $1/a_S$ by scaling the predicted high temperature Δp by a factor λ_p. We also scale a recent prediction for the high temperature bulk viscosity [20] by λ_B. Our best fits give $\lambda_p = 1.07(0.21)$ and $\lambda_B = 0.21(0.60)$. The bulk measurement is consistent with zero, but places a constraint on the maximum value that is within the range of the prediction [20].

This research is supported by the Physics Division of the National Science Foundation (quantum transport in strongly interacting Fermi gases No. PHY-1067873) and by the Division of Materials Science and Engineering, the Office of Basic Energy Sciences, Office of Science, U.S. Department of Energy (thermodynamics in strongly correlated Fermi gases No. DE-SC0008646). Additional support is provided by the Physics Divisions of the Army Research Office (strongly interacting Fermi gases in reduced dimensions No. W911NF-11-1-0420) and the Air Force Office of Scientific Research (non-equilibrium Fermi gases No. FA9550-13-1-0041). The authors are pleased to acknowledge K. Dusling and T. Schäfer, North Carolina State University, for stimulating conversations.

*jethoma7@ncsu.edu

[1] A. Adams, L. D. Carr, T. Schäfer, P. Steinberg, and J. E. Thomas, New J. Phys. **14**, 115009 (2012).
[2] P. K. Kovtun, D. T. Son, and A. O. Starinets, Phys. Rev. Lett. **94**, 111601 (2005).
[3] P. F. Kolb and U. Heinz, *Quark Gluon Plasma 3* (World Scientific, Singapore, 2003), p. 634.
[4] E. Shuryak, Prog. Part. Nucl. Phys. **53**, 273 (2004).
[5] T. Schäfer, Phys. Rev. A **76**, 063618 (2007).
[6] C. Cao, E. Elliott, J. Joseph, H. Wu, J. Petricka, T. Schäfer, and J. E. Thomas, Science **331**, 58 (2011).

[7] C. Cao, E. Elliott, H. Wu, and J. E. Thomas, New J. Phys. **13**, 075007 (2011).
[8] D. T. Son and M. Wingate, Ann. Phys. (Amsterdam) **321**, 197 (2006).
[9] G. Rupak and T. Schäfer, Phys. Rev. A **76**, 053607 (2007).
[10] T.-L. Ho, Phys. Rev. Lett. **92**, 090402 (2004).
[11] J. E. Thomas, J. Kinast, and A. Turlapov, Phys. Rev. Lett. **95**, 120402 (2005).
[12] M. Ku, A. T. Sommer, L. W. Cheuk, and M. W. Zwierlein, Science **335**, 563 (2012).
[13] K. M. O'Hara, S. L. Hemmer, M. E. Gehm, S. R. Granade, and J. E. Thomas, Science **298**, 2179 (2002).
[14] See Supplemental Material at http://link.aps.org/supplemental/10.1103/PhysRevLett.112.040405 for details.
[15] M. Bartenstein, A. Altmeyer, S. Riedl, R. Geursen, S. Jochim, C. Chin, J. H. Denschlag, R. Grimm, A. Simoni, E. Tiesinga *et al.*, Phys. Rev. Lett. **94**, 103201 (2005).
[16] G. Zürn, T. Lompe, A. N. Wenz, S. Jochim, P. S. Julienne, and J. M. Hutson, Phys. Rev. Lett. **110**, 135301 (2013).
[17] D. T. Son, Phys. Rev. Lett. **98**, 020604 (2007).
[18] M. A. Escobedo, M. Mannarelli, and C. Manuel, Phys. Rev. A **79**, 063623 (2009).
[19] Y.-H. Hou, L. P. Pitaevskii, and S. Stringari, Phys. Rev. A **87**, 033620 (2013).
[20] K. Dusling and T. Schäfer, Phys. Rev. Lett. **111**, 120603 (2013).
[21] E. Taylor and M. Randeria, Phys. Rev. A **81**, 053610 (2010).
[22] We include a small correction $|\Delta\langle \mathbf{r}^2\rangle_{\mathrm{Mag}}| < 0.015|\langle \mathbf{r}^2\rangle|$ arising from the curvature in the bias magnetic field, which is subtracted from the $\langle \mathbf{r}^2\rangle$ data to obtain the $\tau^2(t)$ data that is shown in the figure [14].
[23] T.-L. Ho and E. J. Mueller, Phys. Rev. Lett. **92**, 160404 (2004).